where c is the wing chord and K_1 and K_{i_1} are modified Bessel functions as defined in Ref. 3. The Weissinger solution for each component of the spectral decomposition of the loading is, for all practical purposes, indistinguishable from the true lifting surface solution wherein the boundary condition is satisfied at every point on the wing surface.[4] Thus Eq. (3) may be considered the true lifting surface solution for the problem illustrated by Fig. 3.

Results calculated using Eq. (3) are plotted for successively increasing values of vortex separation d on Fig. 4. The limit for d tending to infinity is compared to Hancock's lifting line solution. In regions of rapidly changing upwash the lifting line theory always overestimates the loading. This is because contributions from low-wavelength spectral components of the upwash are overestimated by a factor of two (analogously to lifting line theory's overprediction of the lift carried by low aspect ratio wings in uniform flow). Calculations based on Eq. (3) indicate that for a vortex passing closely over the center section of a very large aspect ratio wing the lifting line solution, Eq. (1), overestimates the magnitude of the rolling moment by a factor of two.

The difference between lifting line and lifting surface results is also proportional to the forward shift in center of pressure from the quarter chord and hence is an indication of section pitching moment.

References

[1] Filotas, L. T., "Vortex Induced Wing Loads," *AIAA Journal*, Vol. 10, No. 7, July 1972, p. 971.

[2] Hancock, G. J., "Aerodynamic Loading Induced on a Two-Dimensional Wing by a Free Vortex in Incompressible Flow," *The Aeronautical Journal of the Royal Aeronautical Society*, Vol. 75, June 1971, pp. 413–416.

[3] Abamowitz, M. and Stegun, I. A., eds., *Handbook of Mathematical Functions*, Dover, New York, 1965.

[4] Filotas, L. T., "Theory of Airfoil Response in a Gusty Atmosphere—Part I, Aerodynamic Transfer Function," Rept. 139, Oct. 1969, Inst. for Aerospace Studies, Univ. of Toronto, Toronto, Canada.

Insensitivity of Single Particle Time Domain Measurements to Laser Velocimeter "Doppler Ambiguity"

DENNIS A. JOHNSON*

NASA Ames Research Center, Moffett Field, Calif.

Nomenclature

b	= radius of unfocused laser beam – $1/e^2$ intensity point
b_0	= radius of focused laser beam – $1/e^2$ intensity point
f_D	= Doppler frequency shift
$\bar{f}_D$	= mean Doppler frequency shift
$F(\omega)$	= frequency spectrum
i	= photomultiplier tube current
l	= beam path length between lens and focal point
t	= time
U	= particle velocity
θ	= angle formed by incident laser beams
ω	= angular frequency
ω_D	= Doppler angular frequency shift
λ	= wave length of laser beam
σ_ω	= standard deviation of Doppler angular frequency
σ_f	= standard deviation of Doppler frequency
$(\sigma_f/\bar{f}_D)_{\text{meas}}$	= nondimensional standard deviation measured
$(\sigma_f/\bar{f}_D)_{\text{amb}}$	= nondimensional standard deviation associated with "Doppler ambiguity"
$(\sigma_f/\bar{f}_D)_{\text{turb}}$	= nondimensional standard deviation associated with turbulence fluctuations

Received December 14, 1972; revision received February 1, 1973.
Index categories: Research Facilities and Instrumentation; Lasers.

* NRC Postdoctoral Research Associate. Associate Member AIAA.

Introduction

EVEN in the case of a uniform laminar flow where a unique Doppler frequency shift should exist, the signal from a laser velocimeter as observed on a spectrum analyzer has a frequency spectrum of significant width. Goldstein and Hagen[1] associated this signal broadening with an uncertainty in the transmitting optics; whereas Pike[2] et al. attributed it to the finite lifetime of the signal as similarly observed in Doppler radar measurements; whence the term "Doppler ambiguity." Subsequently, Edwards[3] et al. have demonstrated that both explanations were correct and in effect equivalent (i.e. the transmitting optics determine the dimensions of the sensing volume and consequently, the signal lifetime; conversely, the signal lifetime defines the transmitting optics). They and others[4,5] have been able to predict analytically the width and shape of the Doppler frequency spectrum for a uniform velocity field as observed in experiments.

In efforts to make laser velocimeter measurements in high-speed gas flows, where high particle concentrations are difficult if not impossible to obtain, a measurement technique[6] has evolved whereby the Doppler frequency shift is obtained from the short-lived signal burst generated by the light scattering of a single particle. More precisely, the Doppler frequency shift is determined by measuring the time interval between zero crossings of the single particle signal after pedestal removal. The purpose of this Note is to show that the measurements obtained in this manner are not affected by the so called "Doppler ambiguity."

Theory

The photomultiplier tube anode current produced by the light scattering of a single particle as it traverses the sensing volume shown in Fig. 1 is given by[4]

$$i = \text{const}\left\{\exp\left[\frac{-2U^2t^2\cos^2(\theta/2)}{b_0{}^2}\right] + \exp\left[\frac{-2U^2t^2\cos^2(\theta/2)}{b_0{}^2}\right]\cos\omega_D t\right\} \quad (1)$$

Here the laser velocimeter is assumed to be operating in the "dual scatter" or "fringe" mode, and for simplicity, the trajectory of the particle has been taken as the path $y = z = 0$. The first term on the right-hand side of Eq. (1), which makes the signal asymmetric with respect to zero, will be referred to as the pedestal.

Performing the Fourier transform of Eq. (1) we have that

$$F(\omega) = \text{const}\left\{\exp -\frac{1}{2}\left[\frac{\omega b_0}{2U\cos(\theta/2)}\right]^2 + \exp -\frac{1}{2}\left[\frac{(\omega-\omega_D)b_0}{2U\cos(\theta/2)}\right]^2 + \exp -\frac{1}{2}\left[\frac{(\omega+\omega_D)b_0}{2U\cos(\theta/2)}\right]^2\right\} \quad (2)$$

The spectrum centered about $\omega = 0$ arises from the pedestal; the other two which are centered about ω_D and $-\omega_D$ represent

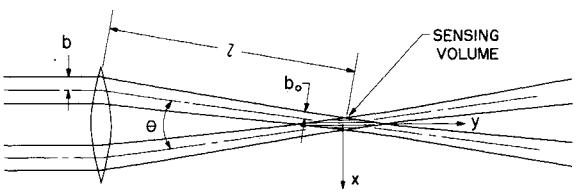

Fig. 1 Schematic representation of interference fringe sensing volume formation.

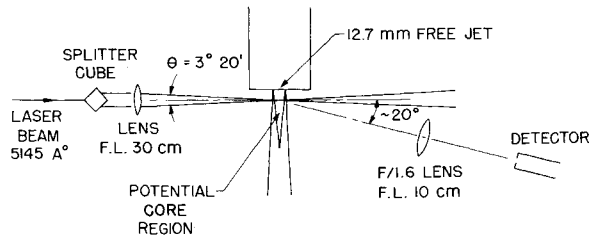

Fig. 2 Schematic representation of optical arrangement of laser velocimeter.

the Doppler spectrum. The relative width $(2\sigma_{\omega}/\omega_D)$ of the Doppler spectrum from Eq. (2) is

$$2\sigma_{\omega}/\omega_D = 2\sigma_f/f_D = (\lambda/\pi b_0)\cot(\theta/2) \tag{3}$$

where the substitution

$$U = \omega_D \lambda/4\pi \sin\theta/2$$

has been made for U. For an ideal lens, b_0 is given by the expression[7]

$$b_0 = (\lambda/\pi)(l/b)$$

Substituting this expression for b_0 into Eq. (3), the more common form[3,4]

$$2\sigma_{\omega}/\omega_D = (b/l)\cot(\theta/2)$$

for the relative spectrum width attributable to the "Doppler ambiguity" is obtained.

Now consider the photomultiplier tube signal, Eq. (1), where by means of a high pass electronic filter the pedestal has been removed to give

$$i = \text{const}\exp -\left[\frac{2U^2t^2\cos^2(\theta/2)}{b_0{}^2}\right]\cos\omega_D t \tag{4}$$

In this case, ω_D is uniquely defined by the zero crossings of the signal. Thus, even though the signal has a frequency spectrum of finite width as given by Eq. (3) due to the finite lifetime of the signal, ω_D can in fact be determined precisely by measuring the time interval between zero crossings of the filtered signal, Eq. (4). That this can be done in practice is shown by the experimental results given in the next section.

Experiment

Doppler frequency measurements by the measurement technique previously described and hot-wire anemometer measurements were taken in the nearly laminar potential core region of a 12.7-mm-diam freejet exhausting air into the ambient. Shown in Fig. 2 is a schematic representation of the laser velocimeter employed and its relation to the freejet. The signal processing arrangement is shown in Fig. 3.

The only signal conditioning performed were 1) the electronic filtering of the pedestal with the high pass filter, and 2) the external triggering of the computing counter by the oscilloscope which allowed only signals with amplitudes above a preset level to be sensed by the counter. The computing counter was programmed to take 1000 measurements and then to compute the mean value and the standard deviation of these measurements. Since the air supplied in the NASA Ames storage tanks was exceptionally clean, it was necessary to seed the flow with tobacco smoke in order to obtain a reasonable data acquisition rate. Care was taken, however, to insure against multiple particle signals—the data acquisition rate was approximately 100 measurements/sec. For this data acquisition rate and the signal lifetimes observed of approximately 10 μsec, the likelihood of a multiple particle signal was less than one in a million. This assumes that the signal occurrences had a Poisson distribution.

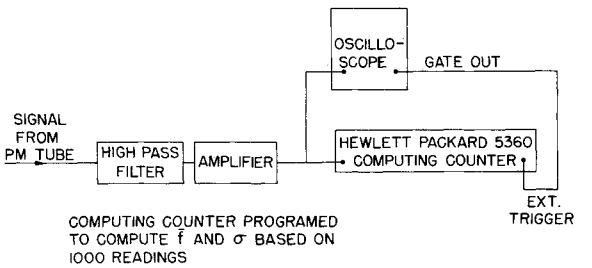

Fig. 3 Schematic representation of signal processing arrangement.

Table 1 Freejet potential core measurements; jet diameter 12.7 mm, downstream distance 6 mm, freestream velocity 17.9 m/sec

Data set[a]	$\bar{f}_D$, MHz	σ_f, kHz	$\sigma_f/\bar{f}_D \times 100$
1	1.976	8.20	0.41
2	1.976	8.18	0.41
3	1.976	8.27	0.42

[a] Each data set based on 1000 measurements.

In the situation where there are variations in the measured Doppler frequency shift due to both turbulence fluctuations and the "Doppler ambiguity," the nondimensional variance in Doppler frequency is given by[1]

$$(\sigma_f/\bar{f}_D)^2_{\text{meas}} = (\sigma_f/\bar{f}_D)^2_{\text{turb}} + (\sigma_f/\bar{f}_D)^2_{\text{amb}}$$

where $(\sigma_f/\bar{f}_D)_{\text{turb}}$ is the turbulence intensity of the flow. For the laser velocimeter configuration employed in this experiment

$$(\sigma_f/\bar{f}_D)_{\text{amb}} = 0.025$$

as determined from Eq. (3). This value corresponds to a θ of 3° 20′, a laser wavelength of 0.5145μ and ab_0 of $115 \pm 5\mu$ as established from oscilloscope traces of the single particle signals. Thus, even in a laminar flow (no velocity fluctuations) the smallest nondimensional standard deviation in Doppler frequency possible with this laser velocimeter arrangement is 2.5% if the "Doppler ambiguity" limits the resolvability of the Doppler frequency shift. However, if the "Doppler ambiguity" has no effect on the measurements, then $(\sigma_f/\bar{f}_D)_{\text{meas}}$ within the accuracy of the measurements represents the turbulence intensity of the flow.

The experimental results for the laser velocimeter obtained along the jet centerline at a downstream distance of 6 mm and a freestream velocity of approximately 18m/sec are given in Table 1. Note that $(\sigma_f/\bar{f}_D)_{\text{meas}}$ was more than a factor of 6 less than $(\sigma_f/\bar{f}_D)_{\text{amb}}$.

Turbulence intensities for the same flow conditions as measured by a hot-wire anemometer ranged from 0.15% to 0.3%. For the low turbulence levels encountered, the hot-wire results are in good agreement with the laser velocimeter measurements. The slightly larger values recorded by the laser velocimeter may have been the result of either inadequate signal-to-noise ratio or pedestal filtering. In any event the measurements were in sufficient agreement to confirm that the laser velocimeter measurements were not affected by the "Doppler ambiguity."

Conclusions

A comparison of hot-wire anemometer and laser velocimeter measurements taken under the same flow conditions confirm that the "Doppler ambiguity" does not affect laser velocimeter measurements obtained by measuring the time interval between zero crossings of single particle signals after pedestal filtering. Thus Gaussian subtraction of the "Doppler ambiguity" broadening $(\sigma_f/\bar{f}_D)_{\text{amb}}$ from the measured nondimensional standard deviation $(\sigma_f/\bar{f}_D)_{\text{meas}}$ to obtain the turbulence intensity is not appropriate in this case. Moreover, since this measurement technique is not affected by the "Doppler ambiguity" there is no ambiguity-limited resolvability of turbulent fluctuations. This is not true for frequency tracker measurements of multiple particle signals.[5]

References

[1] Goldstein, R. J. and Hagen, W. F., "Turbulent Flow Measurements Utilizing the Doppler Shift of Scattered Laser Radiation," *The Physics of Fluids*, Vol. 10, 1967, pp. 1349–1351.

[2] Pike, E. R., Jackson, D. A., Bourke, P. J., and Page, D. I., "Measurement of Turbulent Velocities from the Doppler Shift in Scattered Laser Light," *Journal of Scientific Instruments*, Vol. 1, 1968, pp. 727–730.

[3] Edwards, R. V., Angus, J. C., French, M. J., and Dunning, J. W., Jr., "Spectral Analysis of the Signal from the Laser Doppler Flowmeter: Time-Independent System," *Journal of Applied Physics*, Vol. 42, 1971, pp. 837–850.

[4] Adrian, R. J. and Goldstein, R. J., "Analysis of a Laser Doppler Anemometer," *Journal of Physics*, Ser. E, Vol. 4, 1971, pp. 505–511.

[5] Lumley, J. L., George, W. K., and Yobashi, Y., "The Influence of Ambiguity and Noise on the Measurement of Turbulent Spectra by Doppler Scattering," *Proceedings of the Symposium on Turbulent Measurement in Liquids*, Rolla, Mo., 1969.

[6] Lennert, A. E., Brayton, E. B., Crosswy, F. L., "Summary Report of the Development of a Laser Velocimeter to be Used in AEDC Wind Tunnels," TR-70-101, 1970, Arnold Engineering Development Center, Arnold Air Force Station, Tullahoma, Tenn.

[7] Kognelnik, H., "Imaging of Optical Modes—Resonators with Internal Lenses," *Bell System Technical Journal*, Vol. 44, 1965, pp. 435–494.

Reduction of Structural Frequency Equations

ROBERT L. KIDDER*

Lockheed Missiles & Space Company Inc., Sunnyvale, Calif.

IN determining the natural modes and frequencies of a linearly elastic structure, it is often convenient to reduce the size of the problem by performing a reduction on the mass and stiffness matrices of the governing set of frequency equations. After the modes are determined for the reduced system, it is then necessary to perform a back-transformation to obtain the modes for the entire system; such a procedure is presented in Ref. 1. However, because of the basic assumption in Ref. 1 (a set of forces is assumed to be of zero magnitude), an incorrect expression results for the back-transformation operaton. Presented below is the derivation of the reduction technique which will show the proper back-transformation relationship and what approximations are necessary to obtain the reduced set of frequency equations of Ref. 1.

The partitioned set of equations which define the structural system may be written as

$$\left(-\omega^2\begin{bmatrix}M_{11} & M_{12}\\ M_{21} & M_{22}\end{bmatrix}+\begin{bmatrix}K_{11} & K_{12}\\ K_{21} & K_{22}\end{bmatrix}\right)\begin{Bmatrix}x_1\\ x_2\end{Bmatrix}=\{0\} \quad (1a, b)$$

where ω is the circular frequency, M_{ij} and K_{ij} are submatrices of the mass and stiffness matrices, respectively, and $\{x_1\}$ and $\{x_2\}$ are subvectors of the modal vector $\{x\}$.

Through the use of Eq. (1b) the subvector $\{x_2\}$ may be expressed in terms of the subvector $\{x_1\}$

$$\{x_2\}=-(-\omega^2M_{22}+K_{22})^{-1}(-\omega^2M_{21}+K_{21})\{x_1\} \quad (2)$$

Equation (2) is the required back-transformation relationship, i.e., having determined $\{x_1\}$, $\{x_2\}$ is obtained from Eq. (2) (this back-transformation will be simplified later). Substituting Eq. (2) into (1a) leads to

$$[-\omega^2M_{11}+K_{11}-(-\omega^2M_{12}+K_{12})(-\omega^2M_{22}+K_{22})^{-1}\times(-\omega^2M_{21}+K_{21})]\{x_1\}=\{0\} \quad (3)$$

Equation (3) is the exact reduced set of frequency equations from which the circular frequencies ω and subvectors $\{x_1\}$ could be determined by using an iterative solution technique. However, obtaining solutions from Eq. (3) could be quite time consuming between iteration and obtaining the inverse of $(-\omega^2M_{22}+K_{22})$ for each trial selection of ω.

Another approach to solving Eq. (3) is to expand the inverse term as

$$(-\omega^2M_{22}+K_{22})^{-1}=K_{22}^{-1}+\omega^2K_{22}^{-1}M_{22}K_{22}^{-1}+\cdots \quad (4)$$

where all terms containing ω to higher powers than quadratic are dropped. Inserting Eq. (4) into Eq. (3), and once again dropping the terms which contain the higher powers of ω, yields

$$(-\omega^2M_R+K_R)\{x_1\}=\{0\} \quad (5)$$

where

$$M_R=M_{11}-K_{12}K_{22}^{-1}M_{21}-M_{12}K_{22}^{-1}K_{21}+K_{12}K_{22}^{-1}M_{22}K_{22}^{-1}K_{21} \quad (6)$$

$$K_R=K_{11}-K_{12}K_{22}^{-1}K_{21} \quad (7)$$

The reduced set of frequency equations as defined by Eqs. (5–7) is the same as Ref. 1. The validity of this reduced set of equations rests on the approximation of truncating the expansion of Eq. (4) and the subsequent dropping of terms containing higher powers of ω. As a check on the solution of Eq. (5) the results could be used to see if they satisfy Eq. (3), or the solution of Eq. (5) could be used as a starting point for the solution of Eq. (3).

Once a solution is obtained for the subvectors $\{x_1\}$ and the circular frequencies ω, the remaining portion of the modal vectors $\{x_2\}$ must be calculated from Eq. (2). However, if the values of $\{x_1\}$ and ω are obtained from Eq. (5), then the same approximation of Eq. (4) may be used to simplify the back-transformation to read

$$\{x_2\}=-(K_{22}^{-1}+\omega^2K_{22}^{-1}M_{22}K_{22}^{-1})(-\omega^2M_{21}+K_{21})\{x_1\} \quad (8)$$

The back-transformation of Ref. 1 does not include the inertia terms.

Received December 27, 1972; revision received December 27, 1972. Index category: Structural Dynamic Analysis.

* Staff Engineer, Aeromechanics Department of Space Technology Division.

Reference

[1] Guyan, R. J., "Reduction of Stiffness and Mass Matrices," *AIAA Journal*, Vol. 3, No. 2, Feb. 1965, p. 380.